

Structure and Electronic Properties of Graphene Nanoislands on Co(0001)

Daejin Eom,^{†,‡,§,||} Deborah Prezzi,^{†,‡,⊥} Kwang Taeg Rim,[§] Hui Zhou,^{||}
Michael Lefenfeld,[§] Shengxiong Xiao,[§] Colin Nuckolls,[§] Mark S. Hybertsen,^{*,#}
Tony F. Heinz,^{*,‡,||} and George W. Flynn^{*,‡,§}

Nanoscale Science and Engineering Center, Columbia University, New York, New York 10027, Department of Chemistry, Columbia University, New York, New York 10027, Departments of Physics and Electrical Engineering, Columbia University, New York, New York 10027, INFN-CNR-S3 National Research Center, I-41100 Modena, Italy, and Center for Functional Nanomaterials, Brookhaven National Laboratory, Upton, New York 11973

Received March 24, 2009; Revised Manuscript Received June 16, 2009

ABSTRACT

We have grown well-ordered graphene adlayers on the lattice-matched Co(0001) surface. Low-temperature scanning tunneling microscopy measurements demonstrate an on-top registry of the carbon atoms with respect to the Co(0001) surface. The tunneling conductance spectrum shows that the electronic structure is substantially altered from that of isolated graphene, implying a strong coupling between graphene and cobalt states. Calculations using density functional theory confirm that structures with on-top registry have the lowest energy and provide clear evidence for strong electronic coupling between the graphene π -states and Co d-states at the interface.

Recent successful fabrication of graphene monolayers¹ has attracted a great deal of attention due to the novel physical properties of this material.^{2,3} The high carrier mobility^{2,3} and the possibility of chemical doping^{4,5} make this material a potential building block for future electronic devices. Also, its weak spin-orbit coupling, large phase coherence length, and vanishing hyperfine interaction features suggest that graphene should be a promising medium for spin transport.⁶⁻⁸ Any device applications of this material inevitably involve making contacts to metal electrodes, which can alter the electronic properties of graphene in the contact region⁹⁻¹² and may strongly influence device performance. Hence, unraveling the detailed nature of graphene-metal contacts becomes crucial for successful device fabrication.

While growth of high-quality graphene layers by means of chemical vapor deposition on metal surfaces is rapidly developing,¹³⁻¹⁸ the contact of graphene with Co(0001) and Ni(111) is of particular interest for two reasons. First, the lattice constants of Co(0001) and Ni(111) surfaces match

the in-plane lattice constants of graphene almost perfectly (lattice mismatch <2%).¹⁹ This opens up the possibility of growing stable epitaxial layers without the formation of complex superstructure patterns that are present for large lattice mismatch.^{9,15,20,21} Second, Ni and Co are ferromagnetic metals (FM) that constitute the essential ingredients in spintronic applications.⁸ The recent theoretical study of spin injection characteristics of graphene and graphite samples in contact with Co(0001) or Ni(111) electrodes by Karpan et al.¹⁰ underscores the importance of the registry and the electronic coupling between graphene and the metal surface. Indeed, many theoretical studies, predicting somewhat different results, have been devoted to this issue.^{10,12,22-24} Experimental probes employed to date have been rather limited and also draw different conclusions about graphene registry on Ni(111),^{13,25,26} while registry on Co(0001) has not yet been examined.

Here we report results of a detailed investigation of the structural and electronic properties of well-ordered graphene monolayers grown on the Co(0001) surface. We have determined on-top registry of the graphene layer with respect to the underlying Co lattice. Also, the low-energy electronic structure of the graphene layer was probed by scanning tunneling spectroscopy (STS) and compared with first-principle calculations using density functional theory (DFT). The role of electronic coupling between the graphene π - and the cobalt d-electrons is found to be of particular importance.

* Corresponding authors, mhyberts@bnl.gov, tfh3@columbia.edu, and gwfl@columbia.edu.

[†] Both authors shared equally in the work of this paper. D.E. had major responsibility for the experiments and D.P. had major responsibility for the theoretical calculations.

[‡] Nanoscale Science and Engineering Center, Columbia University.

[§] Department of Chemistry, Columbia University.

^{||} Department of Physics, Columbia University.

[⊥] INFN-CNR-S3 National Research Center.

[#] Center for Functional Nanomaterials, Brookhaven National Laboratory.

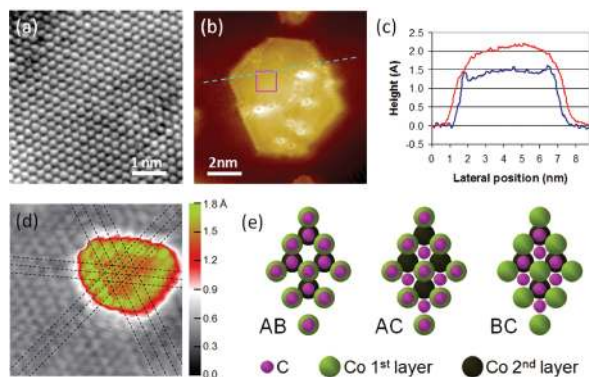


Figure 1. (a–d) Experimental STM topography results: (a) Clean Co(0001) surface (sample bias, $V = +5$ mV). (b) Graphene island grown on Co(0001) ($V = -3$ mV). (c) Height profiles along the dashed line in (b) at $V = -3$ mV (blue), and $V = -400$ mV (red). (d) Small graphene island on Co(0001) ($V = -3$ mV) with guidelines matched to the positions of the Co atoms. Different color scales have been adopted for the substrate and the graphene layer. (e) Three structural models for the registry of graphene on Co(0001).

Our experiments were performed using a low-temperature scanning tunneling microscope (STM) under ultrahigh vacuum (UHV) conditions, at a base pressure of 3×10^{-11} Torr. A cobalt single crystal with (0001) orientation was cleaned in situ by repeated cycles of argon sputtering and thermal annealing at 570 K. Figure 1a shows an STM image of a clean Co(0001) surface with atomic resolution. The cobalt atoms in the image are arranged in a hexagonal pattern with an interatomic distance of 2.5 Å, as expected.¹⁹ The epitaxial graphene islands were grown by thermal decomposition of an adsorbed hydrocarbon precursor. For this purpose, contorted hexabenzocoronene (HBC) molecules²⁷ were deposited onto the clean Co(0001) surface (held at room temperature) by vacuum evaporation from a source at 605 K. The cobalt/hydrocarbon sample was then annealed in situ at 600 K for 20 min, which is well above the dehydrogenation and H₂-desorption temperature (~ 410 K) for hydrocarbons on Co(0001).¹⁴ This procedure resulted in the growth of well-defined, isolated graphene islands, with no evidence for residual, intact HBC molecules. All characterization of the resulting structures was performed by STM at 4.9 K.

Figure 1b illustrates the topography of typical graphene adlayers, which form islands of a few nanometer diameter. While not all of the islands are of regular hexagonal shape, they preferentially exhibit zigzag edges.²⁸ The measured height of the graphene layer above the metal surface varies with the tunneling bias conditions, ranging from ~ 1.5 Å at low tunneling bias (Figure 1c, blue curve) to ~ 2.2 Å at relatively high biases (red curve). Figure 1d displays in more detail the topography of a small graphene island. Under the bias conditions used for Figure 1d, only every second carbon atom in the graphene layer is observed in the image, just as for graphite surfaces.²⁹ This effect is expected to result from the inequivalence of adjacent C atoms in the graphene layer with respect to the underlying Co surface. We have examined the registry of the C atoms through comparison of the STM

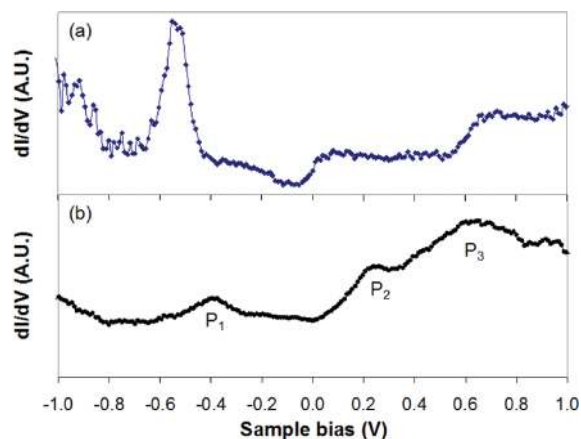


Figure 2. Experimental STS data for differential conductance, dI/dV , for (a) the clean Co(0001) surface and (b) graphene on Co(0001), averaged over the rectangular region shown in Figure 1b, with labels for the main features. All energies are referenced to the Fermi level, E_F .

images above and away from the graphene adlayer. Analysis of the guidelines in Figure 1d shows that the bright features of graphene (except along the edges) are in on-top registry with those of the substrate atoms, demonstrating epitaxial growth on Co(0001). Thus, one of the two carbon atoms in the graphene unit cell is sitting directly above a cobalt atom (on-top site or A-site). The other carbon atom may be located in either an hexagonal close packed hollow site (B-site; see AB model in Figure 1e) or a face-centered cubic hollow site (C-site; see AC model in Figure 1e) of the cobalt substrate. We were not able to obtain images that could distinguish between these two models.

The differential conductance spectrum for the clean Co(0001) surface is shown in Figure 2a. Three principal features can be seen: a strong peak at -0.52 eV, signature of the well-known Co(0001) surface 3d-states of minority-spin character;³⁰ a feature at $+0.1$ eV, characteristic of majority-spin surface states located at the $\bar{\Gamma}$ point of the surface Brillouin zone (BZ);³¹ a feature around $+0.74$ eV, corresponding to either surface or a mixture of surface and bulk states with minority-spin character.³¹ STM measurements performed over the central regions of the graphene islands reveal completely different tunneling spectra from those of the clean Co surface. We have reproduced the experimental spectra with different tips, thereby ruling out any contributions arising from tip artifacts. Figure 2b shows the differential conductance averaged over the rectangular region in Figure 1b, chosen to be well separated from the graphene boundaries and away from any defect.³² Specifically, the grid points over which the $I-V$ curves are sampled encompass at least 23 graphene unit cells with a fine spacing of ~ 0.86 Å, so that the results presented in Figure 2b represent the true spatial average over the two atom (A–B) graphene unit cell. These graphene/Co spectra display three major features at -0.37 eV (designated as P_1), at $+0.25$ eV (P_2), and at $+0.64$ eV (P_3). The graphene/Co STS data are quite different from those of the clean Co(0001) surface; the results are also unlike those of isolated graphene monolayers on oxide surfaces,³³ which are relatively featureless.

We have carried out DFT calculations to find the optimized geometry of graphene on Co(0001) and to analyze its electronic structure. Calculations³⁴ were performed within the local-density approximation (LDA) for the exchange-correlation potential, using a plane-wave basis set and ultrasoft pseudopotentials, as implemented in the Quantum-ESPRESSO package.³⁵ Figure 1e illustrates the geometries tested, which include the above-mentioned AB and AC models as well as the hollow-site geometry (BC model). The binding energies (E_b) indicate that the on-top geometries (AB and AC) are much more stable than the hollow-site BC model, with values of $E_b = 0.255, 0.264,$ and 0.056 eV per C atom pair, respectively. The spacing between the plane of Co atoms and the graphene layer for the on-top geometries was found to be 2.07 Å. While a direct comparison to the nominal height of the graphene islands in the STM topographical traces is not fully justified, the results are consistent with the characteristic heights seen experimentally (~ 1.5 – 2.2 Å, Figure 1c). We note that the separation of graphene from Co(0001) is much smaller than the typical value of 3.3 Å characteristic of graphene on top of other metals like Au, Ag, Cu, or Pt,¹² as a result of a stronger interaction with the Co surface. Indeed, the binding energies for the on-top geometries are clearly greater than those expected for van der Waals interactions alone.

The calculated band structure for the AC geometry is displayed in Figure 3.³⁶ The majority-spin bands (gray) are shown over a broad energy scale in Figure 3a. As the comparison to the downshifted energy-band structure for an ideal graphene sheet in Figure 3a makes clear, the σ bands for graphene on Co(0001) are simply rigidly shifted. However, the apparently intact portions of the π bands below the Co projected band edge are shifted by an additional ~ 1 eV. This reflects the strong electronic coupling of the π bands to the d-states at the Co interface layer. Recent photoemission measurements for the graphene/Ni(111)^{37,38} show similar coupling effects between the metal d-states and the graphene π bands, and a similar hybridization has been reported for graphene/SiC(0001).³⁹ The calculated work function of graphene on Co(0001) for the AC geometry ($W = 3.65$ eV) indicates an apparent n-type doping,⁴⁰ which is consistent with the shift of the σ bands with respect to isolated graphene. Similar values have been recently reported for the calculated work functions.¹²

The carbon contribution to the bands, shown in Figure 3b,c for the two spin channels (red dots), is mainly visible around the K-point. Except in gap regions of the projected band structure, the π bands couple to several Co bands in the slab. Also, the characteristic conical point of the isolated graphene bands is destroyed due to coupling to the metal. The strong interaction with the Co 3d-states is illustrated schematically in Figure 4 for the K-point. Near the K-point, the d_{z^2} states at the Co surface, which tend to concentrate near the top and bottom of the projected energy bands, are mainly coupled to the p_z -orbital located on the A (top) carbon site. The p_z on the C (hollow) site hybridizes with all the other d-type states centered on the three Co atoms surrounding the hollow. In particular, the strongest coupling is with

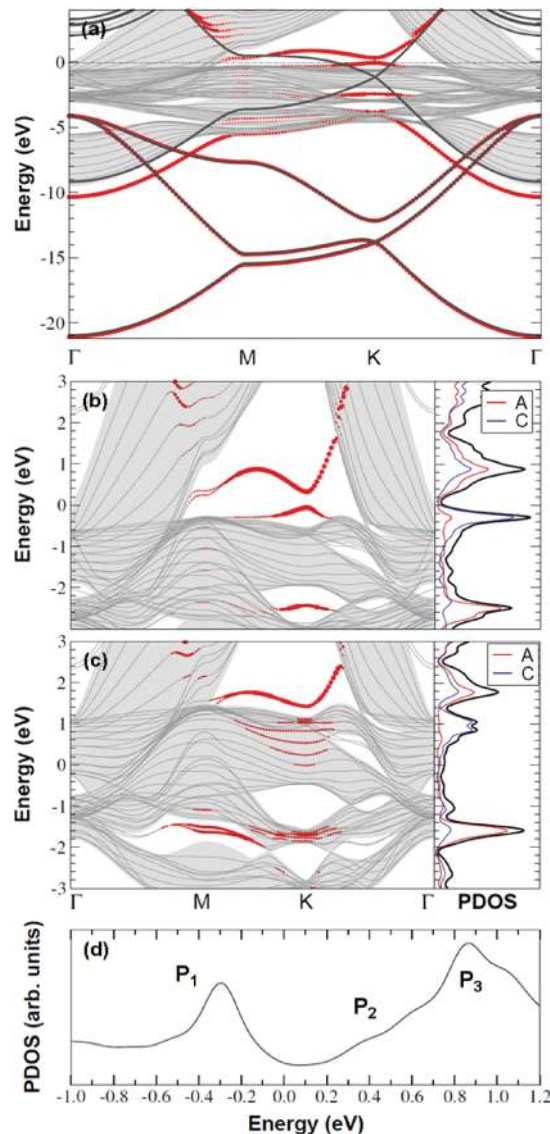


Figure 3. Calculated energy bands and density of states of graphene on Co(0001) in the AC geometry. (a) Majority-spin bands (gray lines, red dots) against the bulk Co(0001) projected bands (shaded area) and the energy bands for ideal graphene downshifted by 1.1 eV (black lines). Size of the red dots is proportional to the projection of the state onto the carbon p_z -orbitals. (b) Detail of (a) near the Fermi energy (left), together with the atom-resolved and total projected DOS (right). (c) Same for minority-spin bands. (d) Spin-integrated PDOS with labels for main features.

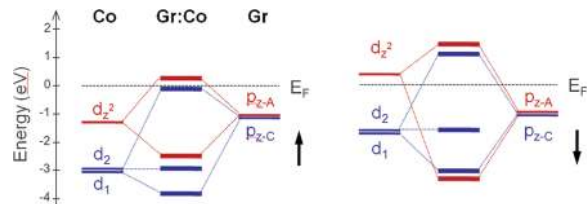


Figure 4. Schematic illustration of the electronic coupling between cobalt d- and carbon p_z -states near the K-point in the surface BZ for majority- and minority-spin states (left and right). Fermi energy indicated.

a pair of surface-localized d orbitals (d_1 and d_2 in Figure 4), which form one linear combination that couples to the C-site p_z orbital, and a second that is passive.

The projected density of states (PDOS) of graphene-derived bands on Co(0001) (Figure 3b,c) are calculated by summing up the projections of each state onto the carbon p_z orbitals. They show the distinct coupling features of Co 3d-states and graphene π -states. The upper majority spin band in Figure 3b results in a peak near 0.8 eV, which derives from the region near the M–K line, where the A- and C-site carbon p_z contributions are mixed. Its analogue for minority spins is located at about 1.7 eV. On the other hand, the prominent majority spin peak at -0.3 eV results primarily from the C-site p_z orbital. The corresponding peak is near 0.8 eV in the minority spin channel. The sum of the projected DOS over the two spin channels is shown in Figure 3d. The structure of the calculated spectrum compares quite well with the experimental one (Figure 2b), with differences in the feature locations of about 0.1–0.2 eV. As we have noted above, these features derive from the edge region of the surface BZ (near the M–K line) and decay more quickly as a function of distance above the surface than the states near the zone center. On the other hand, the states localized near the zone center have very little contribution from the graphene states, giving rise to a featureless partial DOS,⁴¹ which differs markedly from the STS data. For reference, the partial DOS for the clean Co(0001) surface shows a clear feature near -0.5 eV, similar to experiment. Therefore, the comparison of theory and experiments suggests the presence of a mechanism which mixes zone-edge and zone-center states, significantly altering the tunneling current. A similar mechanism, based on electron–phonon coupling, was recently proposed to explain anomalous behavior observed in graphene tunneling spectra.^{42,43}

In conclusion, we have successfully grown epitaxial graphene monolayers on the Co(0001) surface, which have been probed experimentally by STM and compared with DFT calculations. The STM images reveal an on-top registry of C atoms with respect to the underlying Co surface, a picture further corroborated by DFT total energy calculations. Furthermore, the tunneling conductance spectrum of graphene on Co(0001) exhibits several distinct features, in marked contrast to measurements on more isolated graphene samples. As shown from DFT calculations, these features originate from the strong interaction between graphene and Co(0001) d-electrons, as evident also from the disruption of the graphene π -bands. These studies suggest that further control or modification of the interface will be required for transfer of spin-polarized electrons from the ferromagnetic contact into the graphene adlayer.

Acknowledgment. This work was supported by the U.S. Department of Energy (DE-FG02-88-ER13937 to G.W.F., DE-FG02-03ER15463 to T.F.H., and DE-AC02-98CH10886 to M.S.H.), by the National Science Foundation through the NSEC Program (CHE-06-41523), by the New York State Office of Science, Technology, and Academic Research (NYSTAR), and by the “Fondazione Cassa di Risparmio di Modena” (to D.P.). Computing time was provided by CINECA and the Center for Functional Nanomaterials at Brookhaven National Laboratory. Equipment and material

support was provided by the National Science Foundation through Grant CHE-07-01483 (to G.W.F.).

References

- (1) Novoselov, K. S.; Geim, A. K.; Morozov, S. V.; Jiang, D.; Zhang, Y.; Dubonos, S. V.; Grigorieva, I. V.; Firsov, A. A. *Science* **2004**, *306*, 666–669.
- (2) Novoselov, K. S.; Geim, A. K.; Morozov, S. V.; Jiang, D.; Katsnelson, M. I.; Grigorieva, I. V.; Dubonos, S. V.; Firsov, A. A. *Nature (London)* **2005**, *438*, 197–200.
- (3) Zhang, Y.; Tan, Y.-W.; Stormer, H. L.; Kim, P. *Nature (London)* **2005**, *438*, 201–204.
- (4) Liu, L.; Ryu, S.; Tomasik, M. R.; Stolyarova, E.; Jung, N.; Hybertsen, M. S.; Steigerwald, M. L.; Brus, L. E.; Flynn, G. W. *Nano Lett.* **2008**, *8*, 1965–1970.
- (5) Wehling, T. O.; Novoselov, K. S.; Morozov, S. V.; Vdovin, E. E.; Katsnelson, M. I.; Geim, A. K.; Lichtenstein, A. I. *Nano Lett.* **2008**, *8*, 173–177.
- (6) Kane, C. L.; Mele, E. J. *Phys. Rev. Lett.* **2005**, *95*, 226801.
- (7) Berger, C.; Song, Z.; Li, X.; Wu, X.; Brown, N.; Naud, C.; Mayou, D.; Li, T.; Hass, J.; Marchenkov, A. N.; Conrad, E. H.; First, P. N.; de Heer, W. A. *Science* **2006**, *312*, 1911–1916.
- (8) Tombros, N.; Jozsa, C.; Popinciuc, M.; Jonkman, H. T.; van Wees, B. *Nature (London)* **2007**, *448*, 571–574.
- (9) Marchini, S.; Günther, S.; Wintterlin, J. *Phys. Rev. B* **2007**, *76*, 075429.
- (10) Karpan, V. M.; Giovannetti, G.; Khomyakov, P. A.; Talanana, M.; Starikov, A. A.; Zwierzycki, M.; van den Brink, J.; Brocks, G.; Kelly, P. J. *Phys. Rev. Lett.* **2007**, *99*, 176602.
- (11) Huard, B.; Stander, N.; Sulpizio, J. A.; Goldhaber-Gordon, D. *Phys. Rev. B* **2008**, *78*, 121402(R).
- (12) Giovannetti, G.; Khomyakov, P. A.; Brocks, G.; Karpan, V. M.; van den Brink, J.; Kelly, P. J. *Phys. Rev. Lett.* **2008**, *101*, 026803.
- (13) Gamo, Y.; Nagashima, A.; Wakabayashi, M.; Terai, M.; Oshima, C. *Surf. Sci.* **1997**, *374*, 61–64.
- (14) Vaari, J.; Lahtinen, J.; Hautojärvi, P. *Catal. Lett.* **1997**, *44*, 43–49.
- (15) Vázquez de Parga, A. L.; Calleja, F.; Borca, B. M. C. G.; Passeggi, J.; Hinarejos, J. J.; Guinea, F.; Miranda, R. *Phys. Rev. Lett.* **2008**, *100*, 056807.
- (16) Sutter, P. W.; Flege, J.-I.; Sutter, E. A. *Nat. Mater.* **2008**, *7*, 406–411.
- (17) Reina, A.; Jia, X.; Ho, J.; Nezich, D.; Son, H.; Bulovic, V.; Dresselhaus, M. S.; Kong, J. *Nano Lett.* **2009**, *9*, 30–35.
- (18) Kim, K. S.; Zhao, Y.; Jang, H.; Lee, S. Y.; Kim, J. M.; Kim, K. S.; Ahn, J.-H.; Kim, P.; Choi, J.-Y.; Hong, B. H. *Nature (London)* **2009**, *457*, 706–710.
- (19) Wyckoff, R. W. G. *The Structure of Crystals*, 2nd ed.; The Chemical Catalog: New York, 1931.
- (20) Martoccia, D.; Willmott, P. R.; Brugger, T.; Björck, M.; Günther, S.; Schlepütz, C. M.; Cervellino, A.; Pauli, S. A.; Patterson, B. D.; Marchini, S.; Wintterlin, J.; Moritz, W.; Greber, T. *Phys. Rev. Lett.* **2008**, *101*, 126102.
- (21) N’Diaye, A. T.; Bleikamp, S.; Feibelman, P. J.; Michely, T. *Phys. Rev. Lett.* **2006**, *97*, 215501.
- (22) Souzu, Y.; Tsukada, M. *Surf. Sci.* **1995**, *326*, 42–52.
- (23) Bertoni, G.; Calmels, L.; Altibelli, A.; Serin, V. *Phys. Rev. B* **2005**, *71*, 075402.
- (24) Fuentes-Cabrera, M.; Baskes, M. I.; Melechko, A. V.; Simpson, M. L. *Phys. Rev. B* **2008**, *77*, 035405.
- (25) Rosei, R.; De Crescenzi, M.; Sette, F.; Quaresima, C.; Savoia, A.; Perfetti, P. *Phys. Rev. B* **1983**, *28*, 1161–1164.
- (26) Kawanowa, H.; Ozawa, H.; Yazaki, T.; Gotoh, Y.; Souda, R. *Jpn. J. Appl. Phys.* **2002**, *41*, 6149–6152.
- (27) Xiao, S.; Myers, M.; Miao, Q.; Sanaur, S.; Pang, K.; Steigerwald, M. L.; Nuckolls, C. *Angew. Chem., Int. Ed.* **2005**, *44*, 7390–7394.
- (28) The details of the graphene island shape and of the distinctive electronic structure found along the edges will be discussed in a later publication.
- (29) Gwo, S.; Shih, C. K. *Phys. Rev. B* **1993**, *47*, 13059–13062.
- (30) Barral, M. A.; Weissmann, M.; Llois, A. M. *Phys. Rev. B* **2005**, *72*, 125433.
- (31) Math, C.; Braun, J.; Donath, M. *Surf. Sci.* **2001**, *482–485*, 556–561.
- (32) Similar results were obtained for the interior of different islands and the possible effects of quantum confinement do not appear to be appreciable.
- (33) Stolyarova, E. Unpublished results.

- (34) The surface has been modeled in a supercell approach using an 11-layer slab of Co(0001)(1×1) and one layer of graphene on both sides of the slab. The in-plane lattice parameter is set equal to 2.42 Å, i.e., the optimized parameter for bulk Co, and the atomic positions within the cell are fully relaxed.
- (35) Quantum-ESPRESSO is a community project for high-quality quantum-simulation software, based on density-functional theory, and coordinated by Paolo Giannozzi. See <http://www.quantum-espresso.org> and <http://www.pwscf.org>.
- (36) A full characterization of the AB geometry has also been carried out, showing very similar features.
- (37) Varykhalov, A.; Sánchez-Barriga, J.; Shikin, A. M.; Biswas, C.; Vescovo, E.; Rybkin, A.; Marchenko, D.; Rader, O. *Phys. Rev. Lett.* **2008**, *101*, 157601.
- (38) Nagashima, A.; Tejima, N.; Oshima, C. *Phys. Rev. B* **1994**, *50*, 17487.
- (39) Emtsev, K. V.; Speck, F.; Seyller, Th.; Ley, L.; Riley, J. D. *Phys. Rev. B* **2008**, *77*, 155303.
- (40) The calculated work functions for isolated graphene and Co(0001) surfaces are 4.39 and 5.40 eV, respectively.
- (41) Partial DOS (not shown) have been evaluated on planes above the surface, at varying plane–surface distances.
- (42) Zhang, Y.; Brar, V. W.; Wang, F.; Girit, C.; Yayon, Y.; Panlasigui, M.; Zettl, A.; Crommie, M. F. *Nat. Phys.* **2008**, *4*, 627–630.
- (43) Wehling, T. O.; Grigorenko, I.; Lichtenstein, A. I.; Balatsky, A. V. *Phys. Rev. Lett.* **2008**, *101*, 216803.

NL900927F